Published in final edited form as:
J Exp Biol. 2007 February ; 210(Pt 3): 383–394.

Running stability is enhanced by a proximo-distal gradient in joint neuromechanical control

M. A. Daley[*], **G. Felix**, and **A. A. Biewener**
Concord Field Station, MCZ, Harvard University, 100 Old Causeway Road, Bedford, MA 01730, USA

Summary

We currently know little about how animals achieve dynamic stability when running over uneven and unpredictable terrain, often characteristic of their natural environment. Here we investigate how limb and joint mechanics of an avian biped, the helmeted guinea fowl *Numida meleagris*, respond to an unexpected drop in terrain during running. In particular, we address how joint mechanics are coordinated to achieve whole limb dynamics. Based on muscle–tendon architecture and previous studies of steady and incline locomotion, we hypothesize a proximo-distal gradient in joint neuromechanical control. In this motor control strategy, (1) proximal muscles at the hip and knee joints are controlled primarily in a feedforward manner and exhibit load-insensitive mechanical performance, and (2) distal muscles at the ankle and tarsometatarso-phalangeal (TMP) joints are highly load-sensitive, due to intrinsic mechanical effects and rapid, higher gain proprioceptive feedback. Limb kinematics and kinetics during the unexpected perturbation reveal that limb retraction, controlled largely by the hip, remains similar to level running throughout the perturbed step, despite altered limb loading. Individual joints produce or absorb energy during both level and perturbed running steps, such that the net limb work depends on the balance of energy among the joints. The hip maintains the same mechanical role regardless of limb loading, whereas the ankle and TMP switch between spring-like or damping function depending on limb posture at ground contact. Initial knee angle sets limb posture and alters the balance of work among the joints, although the knee contributes little work itself. This distribution of joint function results in posture-dependent changes in work performance of the limb, which allow guinea fowl to rapidly produce or absorb energy in response to the perturbation. The results support the hypothesis that a proximo-distal gradient exists in limb neuromuscular performance and motor control. This control strategy allows limb cycling to remain constant, whereas limb posture, loading and energy performance are interdependent. We propose that this control strategy provides simple, rapid mechanisms for managing energy and controlling velocity when running over rough terrain.

Keywords

running; locomotion; biomechanics; motor control; joint work; joint moment; inverse dynamics

Introduction

We know surprisingly little about how legged animals move with such agility and dynamic stability through their varied and unpredictable natural environments. It appears that all terrestrial animals use similar basic mechanisms for steady movement, despite diversity in size, limb morphology and number of legs (e.g. Cavagna et al., 1977; McMahon and Cheng, 1990; Dickinson et al., 2000; Full and Farley, 2000). However, it is not yet known whether

*Author for correspondence at present address: Division of Kinesiology, University of Michigan, Ann Arbor, MI 48109, USA, (e-mail: mdaley@umich.edu).

different animals use similar neuromuscular control mechanisms to accomplish such strikingly similar function. Furthermore, it is unclear whether the simple models for steady locomotion provide an appropriate framework for understanding how animals control movement over a broader range of conditions. Controlled perturbation experiments can reveal the interplay between mechanics and control, shedding light on these issues and providing groundwork for understanding how animals accomplish such versatile and dynamically stable movement.

Dynamically stable running in varying conditions

A simple mass-spring model accurately describes the stance phase dynamics of bouncing gaits, such as hopping and running, given the appropriate limb parameters (initial limb angle, effective limb length and leg stiffness) and initial conditions (McMahon, 1985; Blickhan, 1989; McMahon and Cheng, 1990; Farley et al., 1993; Schmitt and Holmes, 2000a; Schmitt and Holmes, 2000b; Ghigliazza et al., 2003). Dynamically stable running can be accomplished over a broad range of conditions by adjusting 'leg spring' parameters appropriately (e.g. McMahon and Cheng, 1990; Farley et al., 1993; Full and Farley, 2000). Experimental studies on hopping and running humans have shown that changes in leg stiffness (k_{leg}) help maintain similar body center of mass (COM) motions over surfaces of varying compliance (Ferris and Farley, 1997; Ferris et al., 1998; Ferris et al., 1999; Kerdok et al., 2002). The stability of mass-spring running can be further improved by adjusting initial limb contact angle (Seyfarth et al., 2002), which is accomplished automatically if the limb retracts during late swing phase (Seyfarth et al., 2003). Nonetheless, the mass-spring model is a conservative system, meaning that the total mechanical energy of the body (E_{com}) remains constant. If a perturbation results in a change in one type of mechanical energy, it must be redistributed to another. For example, energy can be redistributed between gravitational potential energy (PE) and kinetic energy (KE) through changes in k_{leg} or initial limb posture (Ferris et al., 1999; Seyfarth et al., 2003). If a movement requires changing the total mechanical energy of the body, the animal must deviate from spring-like mechanics.

Although the mass-spring model is an appropriate starting point for the investigation of running stability, there is no *a priori* reason to expect that the limb will remain a passive 'leg-spring' when its interaction with the environment unexpectedly changes. Even in steady forward running, the muscles at individual joints produce or absorb net energy, achieving spring-like dynamics for whole limb. Proximal joints produce energy, whereas distal joints operate as springs or absorb energy (e.g. Pandy et al., 1988; Belli et al., 2002; Roberts and Scales, 2004). Additionally, the mechanical performance of muscle is sensitive to intrinsic mechanical factors, including muscle and tendon length, shortening velocity and strain history, sometimes called 'preflexes' (Brown and Loeb, 2000). Moreover, limb posture can alter a muscle's mechanical advantage and, consequently, k_{leg} and ground reaction force (GRF) for a given muscle force (McMahon et al., 1987; Biewener, 1989; Biewener, 2003). Consequently, muscle force and work performance can immediately change upon encountering an external perturbation.

On a slower time scale, reflex feedback might also be rapid enough to change muscle activation within the perturbed step (e.g. Nichols and Houk, 1976). Some evidence suggests that reflexes contribute substantially to muscle activity in steady locomotion (reviewed by Grillner, 1975; Pearson et al., 1998; Pearson, 2000). Therefore, both intrinsic mechanical and proprioceptive feedback mechanisms can alter limb dynamics immediately following a perturbation. Since running animals must control their speed and direction in addition to maintaining dynamic stability, the extent to which they will maintain conservative spring-like body motion in rough or unpredictable terrain is not yet clear.

Perturbation experiments reveal strategies for neuromechanical integration

In this paper we explore the neuromuscular and mechanical control strategies used by animals to maintain running stability over uneven terrain by studying the limb and joint dynamics in response to a sudden perturbation. We disrupt the running of helmeted guinea fowl *Numida meleagris* L. by subjecting them to an unexpected drop in substrate height (ΔH) that is camouflaged to remove any visual cue about the upcoming change in terrain. We also compare the unexpected perturbation response to the response when the drop step is visible.

Using this approach, we have previously found that guinea fowl are able to maintain dynamic stability when they encounter a large, sudden drop in substrate height during running (Daley et al., 2006). Nonetheless, the perturbation leads to a number of changes in COM mechanics, examined in detail in the first paper. To summarize briefly, the unexpected perturbation causes a 26±1 ms delay in limb loading relative to that anticipated by the bird (assumed to be the point of tissue paper contact). In the subsequent stance phase, contact time is shortened and mean ground reaction force (GRF) reduced, resulting in a smaller and more variable GRF impulse during stance. The sudden drop in substrate height and decreased weight support following the perturbation causes the body to fall, yielding a net loss in PE. Whether this PE is converted to KE, causing acceleration, or absorbed through negative limb work, preventing acceleration, depends on the magnitude and direction of the ground reaction forces over the course of stance. The birds exhibit three distinct response patterns: (1) KE_h mode, in which the perturbation energy is converted to forward KE, (2) E_{com} mode, in which the perturbation energy is absorbed through negative limb work, and (3) KE_v mode, in which the bird simply falls, converting PE to downward KE (Daley et al., 2006).

Despite the variability in COM mechanics following a drop perturbation, the magnitude and time course of ground reaction forces in the perturbed step can largely be explained by the dynamics of a simple mass-spring model (Daley and Biewener, 2006). Most of the variation in limb loading is associated with altered initial limb contact angle, consistent with the theoretical model (Seyfarth et al., 2003). Nonetheless, the guinea fowl's body mechanics in E_{com} mode trials reveal that, in many cases, the total mechanical energy of the body changes during the perturbed step. This suggests net energy absorption by the hindlimb muscles in some circumstances. In this paper we investigate how body mechanics relate to the underlying limb dynamics following the perturbation. We assess how joint mechanics are coordinated to achieve whole limb function, with particular focus on the implications for neuromechanical control.

Based on muscle–tendon architecture and previous studies of steady and incline locomotion, we hypothesize that a proximo-distal gradient in neuromechanical control is used to coordinate limb function during running. We propose that this control strategy improves stability in rough terrain by causing limb cycling to remain relatively constant, whereas limb energy performance rapidly changes in response to altered interaction between the limb and the ground. In this proximo-distal motor control gradient (1) proximal muscles at the hip and knee joints are controlled in a largely feedforward manner and exhibit load-insensitive mechanical performance, whereas (2) function of distal muscles at the ankle and tarsometatarso-phalangeal (TMP) joints is highly load dependent due to intrinsic mechanical effects and rapid, higher gain proprioceptive feedback. A proximo-distal gradient in muscle function is suggested by studies of limb muscle architecture and *in vivo* muscle performance during steady and incline running (Roberts et al., 1997; Biewener, 1998b; Gillis and Biewener, 2002; Daley and Biewener, 2003; Gillis et al., 2005). Long-fibered proximal muscles modulate limb and body work, whereas short-fibered distal muscles with long tendons favor more economical force generation and elastic energy savings (Biewener and Roberts, 2000). Compared to proximal muscles, we anticipate that muscles at the distal joints are inherently more sensitive to altered loading and exhibit more rapid proprioceptive feedback regulation. The reasons for this are

that (1) the distalmost joints interact directly with the ground and will be the first to encounter and sense changes in terrain, (2) distal muscles may be more sensitive to intrinsic nonlinear contractile effects due to their distinct muscle–tendon architecture, and (3) distal limb joints likely undergo greater intrinsic change in joint dynamics following a perturbation due to the lower inertia of the small distal segments. In contrast, we expect that proximal limb muscles at the hip and knee joints are under greater feedforward control, driven by spinal motor circuits, and relatively insensitive to changes in loading during stance.

We test this proximo-distal control hypothesis by examining the joint moment–angle patterns of running guinea fowl in association with the bird's stabilization response to a sudden, unexpected perturbation involving a drop in substrate height. Based on the reasoning outlined above, we expect the hip and knee to maintain similar mechanical performance as in level running, and the ankle and TMP to undergo rapid changes in kinematics, joint moments and joint work in response to altered limb loading following the unexpected perturbation.

Materials and methods

Animals

We obtained five adult helmeted guinea fowl *Numida meleagris* L., averaging 1.95±0.28 kg body mass, 21±1 cm standing hip height (mean ± s.e.m.) from a local breeder and clipped the primary feathers to prevent them from flying. The ground force data presented here were also reported in the earlier study of body center of mass (COM) mechanics (Daley et al., 2006). Here we measure limb kinematics and use inverse dynamics to investigate joint mechanics following the unexpected perturbation. All of the experimental procedures, individuals and trials are identical to those in the earlier paper. The Harvard Institutional Animal Care and Use Committee approved all procedures. The birds were trained to run on a treadmill and across an 8 m long runway for 1–2 weeks before the experiments. They became accustomed to the runway after 1 or 2 days of training and ran steadily across it at a preferred speed around 3 m s^{-1}. To allow visualization of limb segments, we plucked the bird's feathers to above the hip while it was under anesthesia delivered through a mask (isoflurane, 3% induction, 1–2% maintenance). The joint centers of rotation were found by palpation and marked with high contrast ink.

Experimental procedures and data collection

All experimental procedures and data collection have been described previously (Daley et al., 2006). Briefly, running trials were conducted on an 8 m long runway with Kistler force plate (model 9281A, Amherst, NY, USA) placed at the midway point. The sidewalls in the middle 1.8 m were constructed of 6 mm Plexiglass™ to allow recording of lateral view high-speed digital video. In 'Control' trials (C), the bird ran steadily across the level runway. In 'Unexpected Drop' trials (U), the runway was elevated relative to the force-plate, to create a drop in substrate height (ΔH=8.5 cm) that was disguised by tissue paper pulled tightly across the gap (Fig. 1). The tissue paper broke at a relatively low force of 6 N (approximately 30% of the bird's body weight), and took 16±4 ms to break, exerting a negligible impulse on the COM (Daley et al., 2006). The U trials were randomized to prevent habituation by placing a 6 mm thick white board over the drop between trials and running the bird along a level runway. We conducted no more than 2 or 3 U trials on a given recording day, randomized among 15–20 level trials. At the end of the experiment, we conducted 'Visible Drop' trials (V), in which the bird encountered the same ΔH as in U trials, but could see the upcoming change. We found no evidence of a learning trend in sequential hidden drop trials when kinematic variables were compared using repeated-measures analysis of variance (ANOVA), whereas behavior differed markedly when the birds were allowed to see the upcoming ΔH (V trials) (Daley et al.,

2006). The V trials allow a general comparison to the hidden drop, to provide insight into the effect of removing visual feedback.

Data acquisition and measurements

Ground reaction forces (GRF), measured in the vertical (f_v) and fore–aft (f_h) directions, were recorded at 5000 Hz and synchronized to high-speed digital video recorded in both lateral views at 250 Hz (Redlake Motionscope PCI 500, Cheshire, CT, USA). Force plate data were low pass filtered using a zero-phase fourth-order digital Butterworth filter with a cut-off frequency between 90–100 Hz.

Kinematic points located at the middle toe, tarsometatarsophalangeal joint (TMP), ankle, knee, hip, synsacrum and the approximate body COM were digitized, smoothed and interpolated to 5000 Hz as described previously (Daley et al., 2006). We calculated joint angles (Fig. 2), relative limb length (L/L_t, where L is the distance between the hip and toe, and L_t is the sum of all limb segment lengths), and limb angle (θ), the angle of the line between hip and toe, relative to horizontal (Fig. 1, Table 1).

Average limb stiffness (k_{leg}) was calculated over the duration of the limb compression (decrease in leg length during an increase in GRF). Thus, k_{leg} was the change in force divided by the change in length during the limb compression phase of stance. Because there was substantial size variation among the birds in the study (Table 1), we normalized this k_{leg} as a dimensionless stiffness ($K_{leg}=k_{leg}L_t\ mg^{-1}$) (McMahon and Cheng, 1990) to account for the scaling of stiffness with body size (Farley et al., 1993). It is important to note that the limb stiffness calculated in this study is not equivalent to the effective virtual ‘leg spring’ stiffness calculated by McMahon and Cheng (McMahon and Cheng, 1990), which assumes a simple mass-spring model and uses length changes between the COM and the point of application of the GRF. During unsteady behaviors, as investigated here, the collective performance of the body and limb may or may not maintain spring-like function. Therefore, we used this measure of k_{leg} to quantify the compressive limb stiffness following the perturbation, to avoid potentially incorrect assumptions about the mechanics of locomotion during unsteady movement. Nonetheless, it is important to note that if limb performance follows steady, spring-like dynamics, the k_{leg} calculated here would be equal to that obtained using the method in previous studies.

We calculated the external moment and work at each joint over the course of stance using inverse dynamics. We did not include internal moments (segment inertial and gravitational terms) because we were concerned with relating joint dynamics to body COM mechanics rather than obtaining accurate values of total muscle work. The external moment is the magnitude of the cross product between the instantaneous joint position vector **P** and the instantaneous GRF vector $\mathbf{F_g}$, where **P** is composed of the x and y distances between the force plate center of pressure (COP; Fig. 2) and the center of rotation for each joint, and $\mathbf{F_g}$ is composed of the x and y components of the GRF. By convention, an extensor moment and an extending angle change were positive. The joint moment and joint angular velocity were multiplied at each time point to obtain joint power. Joint work was calculated by numerical integration of joint power over time. Using this approach, the value of work at the last time point of stance is the net external work done by that joint. We also calculated the absolute external work done at each joint using the same method, except that we took the absolute value of joint power before integration. Net limb work and absolute limb work were obtained by summing the respective values across all joints in the limb. Together, these two values (net and absolute limb work), also allow calculation of the total negative and positive external limb work. The mean absolute difference in net limb work calculated through inverse dynamics *versus* COM energy analysis (integration of force plate data) (Daley et al., 2006) was 0.08+0.01 J, which is 6% of the average

total external limb work done. All work values were normalized for size by dividing by the bird's body mass.

Statistical analysis

For statistical analysis all mechanical variables were made dimensionless by normalizing to body mass, the acceleration of gravity (***g***) and total limb length (L_t) (McMahon and Cheng, 1990). We subdivided the U trials into three categories corresponding to COM energy response modes (KE_h mode, E_{com} mode, and KE_v mode) (Daley et al., 2006). A two-way ANOVA was used to assess the effect of individual and 'behavior category' (C, U_{KEh}, U_{Ecom}, U_{KEv}, V), on limb angle at ground contact (θ_i), effective limb length at contact (L_i/L_t), leg stiffness (K_{leg}) and average limb retraction rate during stance ($\Delta\theta/T_c$). A two-way ANOVA was also used to assess the effect of individual and 'behavior category' on net joint work and initial limb angle at each joint (Hip, Knee, Ankle, TMP). We used the Tukey Honestly Significant Difference *post hoc* test (THSD) or sequential Bonferroni correction for multiple comparisons. Statistical tests were performed using Systat (version 10.2 for the PC). Unless otherwise stated, we report average values as the mean ± s.e.m.

Results

Changes in limb dynamics during unexpected and visible substrate height perturbations

In our analysis here, we found that the variation in COM mechanics during the perturbed step related to the posture of the limb when it contacted the ground (Fig. 3), as described in detail below. During the time between false floor and ground contact, the limb was unloaded. Despite altered loading, the limb retracted at the same average rate as in level running, although it varied somewhat during the perturbation (C *vs* U, P=0.128 THSD, Fig. 4A). Limb retraction during the substrate drop resulted in a steeper limb angle at the point of ground contact (θ_i; P<0.001 THSD; Fig. 5, Table 2).

As a consequence of unloading during the perturbation, the limb did not compress as it normally does during the beginning of stance (Fig. 3). During the tissue break-through phase, the limb exhibited varying degrees of flexion and extension (Fig. 4B). In the stance phase following the ΔH, it extended for a short period at the beginning of stance before compressing (Fig. 4B). The U perturbations consistently exhibited this pattern of limb extension early in stance, which differed markedly from the leg compression–extension cycle seen in level running. However, we did not observe a similar pattern during V perturbations. In visible substrate drops the limb also contacted the ground with a steeper angle (Fig. 5, Table 2). However, the limb was more extended upon contact and began compression immediately (Fig. 4B).

The relationship between limb posture and body mechanics

Limb contact angle (θ_i), initial relative limb length (L_i/L_t), and limb stiffness (K_{leg}) all varied considerably among the unexpected perturbations (Fig. 5). Yet, only the variation in initial limb posture (θ_i and L_i/L_t) significantly differed among response modes, whereas K_{leg} did not (Table 2). Limb stiffness varied among individuals, but did not differ significantly across behavior categories (Table 2). Therefore, K_{leg} did not appear to play a major role in distinguishing limb dynamics among the behavior categories. In contrast, initial limb angle (θ_i) and initial relative limb length (L_i/L_t) differed significantly among perturbation response modes. Initial limb angle (θ_i) was significantly higher in KE_v perturbation responses (P=0.013), whereas L_i/L_t tended to be longer in E_{com} responses (P=0.039; Fig. 5D, 'ΔE_{com} mode'). Thus, limb posture (θ_i and L_i/L_t) significantly distinguished the three perturbation response modes. When the limb contacted the ground with an extended posture, it absorbed the perturbation energy through negative limb work. At intermediate θ_i and L_i/L_t the limb converted the

perturbation energy to KE_h. When the limb contacted the ground with a very steep angle, the limb exerted little force on the ground and the bird simply fell, converting PE to KE_v.

The contribution of individual joints to limb mechanical function

The individual joints of the limb performed distinct roles during level running (Fig. 6). The hip produced positive work while extending. The knee flexed rapidly under a low moment and maintained a relatively constant angle at higher moments, performing little net work. The ankle primarily operated in a spring-like manner, absorbing and returning energy (although it absorbed a small amount of energy on average). The TMP joint acted as a damper, absorbing net energy. The positive work produced by the hip was balanced by energy absorption at the TMP, resulting in zero energy change for the whole limb (Fig. 7C, Fig. 8), as expected for steady level running.

In the perturbed trials, the magnitude of the work done at each joint decreased with increasing limb contact angle (Fig. 7; $P<0.001$ for all individual joints *vs* θ_i). There was also a dramatic decrease in absolute limb work with increasing θ_i (Fig. 7C). However, net energy produced by the limb depended on the balance among the joints, and net limb work did not exhibit a significant linear relationship with θ_i (Fig. 7C).

In association with altered limb loading following the perturbation, the torques at each joint often briefly reversed at the beginning of stance (Fig. 6, middle panels). Otherwise, the overall patterns of joint torques did not substantially differ from level running, apart from more rapid rise and fall, and shorter duration. The exceptions to this were KE_v mode trials (3 of 19 U trials), in which the peak moments were greatly reduced in magnitude and duration (Fig. 6, green broken lines).

The U perturbations affected the mechanics at each joint differently. Despite altered loading, the proximal joints retained similar overall function as during steady running. The hip extended to a similar extent as in control trials, and consistently produced positive work under extension, although the amount of work done varied among U response modes (Fig. 6A, Fig. 7A). Whereas knee kinematics varied substantially, net work performed at the knee remained near zero in all cases because it underwent little angular change during periods of high torque (Fig. 6B, Fig. 7A).

In contrast, the function of the ankle and TMP joints depended on the posture of the limb at the point of ground contact. Both of these joints acted as dampers (absorbing energy) under some circumstances and as springs (absorbing and returning energy) under other circumstances (Fig. 6C,D, Fig. 7B). When the limb contacted the ground with an extended posture and shallower angle, these two distal joints absorbed net energy, whereas when the limb contacted the ground with a crouched posture and steeper angle, they operated in a springlike manner with little net work (E_{com} mode *vs* KE_h mode, respectively). When limb contact angle was very near vertical, the forces on the limb were too low to exert substantial joint moments, and neither of these joints performed substantial work (KE_v mode).

Thus, the balance of work among the joints related to the posture of the limb at the time of ground contact. Consequently, we were interested in understanding how overall limb posture related to the configuration of the joints at contact. Surprisingly, the variation in initial limb posture related only to the initial knee angle. The hip and ankle were consistently more extended at contact following the perturbation than during level running (Hip, $P=0.014$; Ankle, $P<0.001$; Fig. 6, left panel). However, this did not differ among the different U response modes. The TMP angle did not differ from control trials at the point of ground contact (Fig. 6D, left panel). In contrast, the knee sometimes flexed and sometimes extended following tissue break through, resulting in a variable joint angle at ground contact (Fig. 6B, left panel). The knee was the only

joint that differed among the U response modes (P=0.008), landing in a significantly more extended position in E_{com} mode (P=0.047) and a significantly more flexed position in KE_v mode (P=0.006). Therefore, the variation in limb posture that distinguishes the different U response modes resulted from variation in knee angle at the time of ground contact (Fig. 9).

Discussion

Limb mechanics in relation to the mass-spring model

Here we examine the limb and joint mechanics following a sudden, unexpected drop in substrate height to reveal the neuromechanical control mechanisms used by guinea fowl to maintain running stability. To deal with a sudden change in substrate height, an animal can (1) rapidly adjust its 'leg-spring' to prevent changes in mechanical energy, (2) redistribute energy between PE and KE, or (3) actuate the limb to change E_{com} (for example, absorbing energy to maintain the same velocity at the lower substrate height). A simple mass-spring system can accomplish only the first two of these. In an earlier study using the same experimental perturbation, we found that guinea fowl are remarkably successful in maintaining dynamic stability of their COM motion in response to this perturbation (Daley et al., 2006). However, the COM mechanics during the perturbed step vary dramatically. The birds exhibit three response patterns: E_{com} mode, in which the limb absorbs energy, preventing acceleration, KE_h mode, in which the bird accelerates forward in response to the perturbation, and KE_v mode, in which the limb does not exert substantial force and the body simply falls, converting PE to vertical KE (Daley et al., 2006). Here we show that these response modes result from the interplay between initial limb posture and individual joint work performance during the stance phase following the unexpected perturbation.

Control of running stability through a mass-spring template

To a large extent, the guinea fowl's response to the unexpected ΔH perturbation is consistent with the mass-spring model. Most of the variation in limb loading can be explained by the effect of limb contact angle on 'leg spring' loading during stance (Daley and Biewener, 2006), consistent with the theoretical running model proposed by Seyfarth and colleagues (Seyfarth et al., 2002; Seyfarth et al., 2003). Likewise, the decrease in the magnitude of work done at each joint with increasing θ_i (Fig. 7) can be viewed as a consequence of the inverse relationship between θ_i and leg-spring loading.

Nonetheless, even during level running, the spring-like dynamics of the whole body arise through a balance of positive and negative work among the limb joints, rather than through actual elastic energy storage at each joint (Fig. 6), although some elastic storage occurs at the ankle and TMP during level running (Daley and Biewener, 2003). Net energy production at the hip offsets energy absorption at distal joints (Figs 6 and 7). This suggests that the guinea fowl does not fully benefit from the efficiency of a truly elastic system. However, the results are consistent with the idea that the mass-spring model represents a true control target of the neuromechanical system (e.g. Ferris and Farley, 1997;Ferris et al., 1999;Moritz and Farley, 2004). By controlling the limb around a mass-spring control template (e.g. Full and Koditschek, 1999;Koditschek et al., 2004), the bird might simplify neuromuscular control by reducing the complexity of the system to a few controllable limb parameters.

Stabilization at different energy states through posture-dependent limb actuation

When the limb moves away from its normal posture, the balance of energy among the joints is altered, and the limb produces or absorbs net energy. This posture-dependent limb actuation appears to relate to initial knee angle (Fig. 9). When the limb contacts the ground with an extended knee, resulting in a lower limb contact angle (θ_i) and longer initial relative length (L_i/L_t), the distal joints (ankle and TMP) act as dampers (E_{com} mode, Figs 6 and 8). This shifts

the energy balance among the joints, resulting in net energy absorption, and the bird does not accelerate as a result of the energy gained from the perturbation. In contrast, when the limb contacts the ground with a flexed knee, resulting in a higher θ_i and shorter L_i/L_t, the distal joints act as springs (KE_h mode, Figs 6 and 8). Consequently, the net limb work is positive, and the bird accelerates. Thus, depending on the limb posture at contact, the bird either absorbs energy and stabilizes at the original velocity, or accelerates and stabilizes at a higher velocity. A mass-spring system can achieve stable running at many different periodic trajectories (Taga et al., 1991;Full et al., 2002;Koditschek et al., 2004). Posture-dependent actuation of the guinea fowl's limb provides a simple mechanism for switching among stable periodic trajectories with different energies (i.e. different COM height and/or velocity). This allows rapid control of limb posture and forward velocity when running over rough terrain.

Neuromuscular control of limb function during running

The neuromuscular mechanisms used to coordinate steady running influence the mechanical response when the limb's interaction with the ground suddenly changes. A muscle's mechanical performance depends on its activation pattern as well as its intrinsic mechanical environment, due to the nonlinear contractile properties of muscle tissue (reviewed by Josephson, 1999; Marsh, 1999). A muscle's activation timing and intensity depends on a combination of rhythmic, feedforward control, proprioceptive feedback (reviewed by Grillner, 1975; Pearson et al., 1998; Pearson, 2000). Additionally, muscle–tendon architecture influences a muscle's sensitivity to intrinsic mechanical effects (e.g. Brown and Loeb, 2000; Alexander, 2002), which likely influences how it is controlled by the nervous system. The relative contribution of feedforward, reflex feedback and intrinsic mechanical control to muscle performance is not well established, even for steady forward locomotion.

Due to the complex interaction between neural and intrinsic mechanical factors in muscle performance, it is likely that there is an inherent link between a muscle's architecture and the neural control strategy used to activate it. *In vivo* muscle performance during level and incline treadmill running suggest a proximo-distal gradient in muscle mechanical function (Roberts et al., 1997; Biewener, 1998a; Gillis and Biewener, 2002; Daley and Biewener, 2003; Gillis et al., 2005). Distal hindlimb muscles tend to have a distinct muscle–tendon architecture with short muscle fibers and long tendons (Biewener, 1998b). This architecture favors economical force generation and elastic energy savings, whereas long-fibered proximal muscles modulate limb and body work (Biewener and Roberts, 2000). Inherently linked with this morphological and functional gradient, we hypothesize that limb muscles are coordinated through a proximo-distal gradient in neuromechanical control. In this control gradient, proximal hindlimb muscles are under greater feedforward control, driven by spinal motor circuits, and relatively insensitive to changes in loading during stance. In contrast, distal muscles undergo more rapid, higher gain proprioceptive feedback regulation and experience greater intrinsic mechanical effects on performance. The distal limb segments are the first to interact with the ground, allowing them to receive rapid proprioceptive feedback. The short fibers of distal muscles might be particularly sensitive to intrinsic changes in force–length performance following a perturbation, due to the nonlinear contractile properties of muscle tissue (reviewed by Josephson, 1999; Marsh, 1999). Additionally, due to their long tendons, tendon elasticity will have a greater impact on the dynamics of distal muscle contraction (Biewener and Roberts, 2000; Alexander, 2002; Roberts, 2002), possibly further enhancing intrinsic mechanical effects. Finally, distal muscles act upon smaller limb segments with lower inertia, likely making distal joints relatively susceptible to intrinsic mechanical changes in response to perturbations. These mechanical properties of distal muscles might cause them to exhibit more rapid and pronounced changes in mechanical performance following a perturbation compared to proximal muscles. Because distal muscles likely experience shorter mechanical time delays in their response to a perturbation, the nervous system could operate them with a higher

proprioceptive feedback gain. Based on these observations, we predict a proximo-distal gradient in motor control that is tightly coupled to the morphological and functional gradient of limb muscles.

The joint mechanics following the unexpected perturbation are consistent with the proposed proximo-distal gradient in joint neuromechanical control. Limb retraction remains largely unchanged in response to the unexpected break-through perturbation (Fig. 4). The hip primarily controls limb retraction, maintaining a similar movement pattern and work performance in C and U trials (Fig. 6). This suggests that the hip extensors are activated primarily in a feedforward manner and relatively insensitive to limb loading. This result is consistent with previous work that suggests that activity of some stance phase muscles is maintained until the hip reaches a certain angle (reviewed by Grillner, 1975;Pearson et al., 1998).

In contrast, distal joint mechanics exhibit greater load dependence, which suggests higher proprioceptive feedback gain and greater sensitivity to intrinsic mechanical factors. Like the hip, the ankle is more extended at contact (Fig. 6), suggesting that ankle extensors are also activated in a feedforward manner. However, the extension of the ankle at the beginning of stance is a reversal of its normal motion, and the work performance of the ankle switches between spring-like and energy absorbing, depending on limb posture at contact (Fig. 6). This suggests that ankle extensor force-length performance depends on how the limb is loaded during stance. Recent evidence suggests that positive force feedback through Golgi tendon organs plays an important role in the regulation muscle activity for weight support during stance (Gorassini et al., 1994;Hiebert et al., 1994;Donelan and Pearson, 2004). The observed pattern of early ankle extension followed by springlike action is consistent with a combination of feedforward activation in anticipation of stance followed by proprioceptive feedback regulation of activation level over the course of stance.

The TMP angle at the start of ground contact is not altered in response to the perturbation (Fig. 6), suggesting that the activation of TMP extensors (i.e. the digital flexors) is highly load dependent. As the most distal muscles, the digital flexors are likely to be the first muscles to sense a change in the interaction between the limb and ground. Consequently, they might respond rapidly to proprioceptive feedback. Additionally, the performance of these distal muscles may be particularly sensitive to intrinsic mechanical factors such as length, velocity, strain history and gearing. In an *in vivo* study of muscle performance, the guinea fowl digital flexor muscle exhibited substantial changes in work that were not associated with altered electromyographic intensity or duration (Daley and Biewener, 2003). Instead, differences in muscle strain in relation to activation pattern influence the digital flexors mechanical performance, suggesting that ‘preflexes’ (Brown and Loeb, 2000) are an important component of control for this muscle. This warrants further study to evaluate how proprioceptive feedback and intrinsic mechanical effects interact to provide rapid and robust control of these important distal muscles.

The knee exhibits variable motion that sets the overall limb configuration and substantially influences limb mechanics (Fig. 9). Yet, it contributes little work itself because it flexes under low moments and remains relatively stationary at higher moments (Fig. 6). The close alignment of the knee to the COM likely allows this joint to reorient the distal limb without substantially altering the torques it must resist during stance (Figs 6, 9). The variable motion at the knee joint likely reflects altered force balance among the multi-articular muscles that cross it. Some of this variation might result from differences in loading during the tissue break-through phase of the perturbation (due to variation in breaking force of the tissue, for example). Although the tissue forces were quite small, they could elicit proprioceptive feedback that would alter subsequent muscle activation. The hip and ankle extensors might respond differently to variation in loading during the tissue break-through phase, due to different proprioceptive

feedback gain or intrinsic mechanical sensitivity. If so, their force balance would be altered, leading to altered knee kinematics and limb configuration. Unfortunately, in the current experiment we were unable to measure the forces exerted on the tissue during the perturbation, so we are unable to fully investigate this issue.

Conclusions

The limb and joint mechanics following an unexpected drop in substrate height suggest a proximo-distal gradient in neuromechanical control in which (1) hip extensors are controlled in a largely feedforward manner and insensitive to load, (2) ankle extensors and digital flexors are highly load dependent due to higher proprioceptive feedback gain and sensitivity to intrinsic mechanical effects and (3) knee posture reflects the force balance among proximal and distal extensor muscles. Under this control strategy, limb cycling remains constant, but limb posture, loading and energy performance are interdependent. The proposed proximo-distal gradient in motor control could explain the observed posture-dependent work performance of the limb, which likely improves running stability by allowing rapid adjustment of limb posture and forward velocity when running over rough terrain.

Acknowledgements

We would like to thank Pedro Ramirez for animal care, and Craig McGowan, Polly McGuigan, Jim Usherwood and Chris Wagner and for helpful discussions and assistance in data collection. We also thank two anonymous referees whose careful reviews helped improve the manuscript. This work was supported by a HHMI Predoctoral Fellowship to M.A.D. and a grant from the NIH (R01-AR047679) to A.A.B.

Glossary

C
: control trials (level running)

COM
: center of mass

COP
: center of pressure

E_{com}
: total body COM energy

ΔE_{limb}
: net external work done by the limb, calculated from inverse dynamics

F_g
: instantaneous ground reaction force vector

$F_{g\ mean}$
: average GRF during stance

f_v
: instantaneous vertical ground reaction force

f_h
: instantaneous fore–aft ground reaction force

GRF
: ground reaction force

g

	gravitational constant
ΔH	change in substrate height
HH	standing hip height
KE_h	horizontal kinetic energy
KE_v	vertical kinetic energy
k_{leg}	limb compressional stiffness
K_{leg}	dimensionless k_{leg} [$K_{leg}=k_{leg}L_t\ (mg)^{-1}$]
L	distance between hip and toe
L_t	total leg length as Σl_{seg}, the sum of leg segment lengths
L/L_t	relative leg length
L_i/L_t	initial relative leg length
P	instantaneous joint position vector
PE	gravitational potential energy
s_v	vertical position of the COM
t_c	duration of ground contact
T_c	dimensionless duration of contact ($t_c/L_t^{1/2}$)
TMP	tarsometatarsophalangeal
U	unexpected substrate drop trials
V	visible substrate drop trials
θ	leg angle relative to horizontal

θ_i initial leg angle relative to horizontal

References

Alexander RM. Tendon elasticity and muscle function. Comp Biochem Physiol 2002;133A:1001–1011.

Belli A, Kyrolainen H, Komi PV. Moment and power of lower limb joints in running. Int J Sports Med 2002;23:136–141. [PubMed: 11842362]

Biewener AA. Scaling body support in mammals: limb posture and muscle mechanics. Science 1989;245:45–48. [PubMed: 2740914]

Biewener AA. Muscle function in vivo: a comparison of muscles use for elastic energy savings versus muscles used to generate mechanical power. Am Zool 1998a;38:703–717.

Biewener AA. Muscle-tendon stresses and elastic energy storage during locomotion in the horse. Comp Biochem Physiol 1998b;120B:73–87.

Biewener, AA. Animal Locomotion. New York: Oxford University Press; 2003.

Biewener AA, Roberts RJ. Muscle and tendon contributions to force, work, and elastic energy savings: a comparative perspective. Excerc Sport Sci Rev 2000;28:99–107.

Blickhan R. The spring mass model for running and hopping. J Biomech 1989;22:1217–1227. [PubMed: 2625422]

Brown, IE.; Loeb, GE. A reductionist approach to creating and using neuromechanical models. In: Winters, JM.; Crago, PE., editors. Biomechanics and Neural Control of Posture and Movement. New York: Springer-Verlag; 2000. p. 148-163.

Cavagna GA, Heglund NC, Taylor CR. Mechanical work in terrestrial locomotion: two basic mechanisms for minimizing energy expenditure. Am J Physiol 1977;233:R243–R261. [PubMed: 411381]

Daley MA, Biewener AA. Muscle force–length dynamics during level *versus* incline locomotion: a comparison of *in vivo* performance of two guinea fowl ankle extensors. J Exp Biol 2003;206:2941–2958. [PubMed: 12878663]

Daley MA, Biewener AA. Running over rough terrain reveals limb control for intrinsic stability. Proc Natl Acad Sci USA 2006;103:15681–15686. [PubMed: 17032779]

Daley MA, Usherwood JR, Felix G, Biewener AA. Running over rough terrain: guinea fowl maintain dynamic stability despite a large unexpected change in substrate height. J Exp Biol 2006;209:171–187. [PubMed: 16354788]

Dickinson MH, Farley CT, Full RJ, Koehl MAR, Kram R, Lehman S. How animals move: an integrative view. Science 2000;288:100–106. [PubMed: 10753108]

Donelan JM, Pearson KG. Contribution of force feedback to ankle extensor activity in decerebrate walking cats. J Neurophysiol 2004;92:2093–2104. [PubMed: 15381742]

Farley CT, Glasheen J, McMahon TA. Running springs: speed and animal size. J Exp Biol 1993;185:71–86. [PubMed: 8294853]

Ferris DP, Farley CT. Interaction of leg stiffness and surface stiffness during human hopping. J Appl Physiol 1997;82:15–22. [PubMed: 9029193]

Ferris DP, Louie M, Farley CT. Running in the real world: adjusting leg stiffness for different surfaces. Proc R Soc Lond B Biol Sci 1998;265:989–994.

Ferris DP, Liang K, Farley CT. Runners adjust leg stiffness for their first step on a new running surface. J Biomech 1999;32:787–794. [PubMed: 10433420]

Full, RJ.; Farley, CT. Musculoskeletal dynamics in rhythmic systems: a comparative approach to legged locomotion. In: Winters, JM.; Crago, PE., editors. Biomechanics and Neural Control of Posture and Movement. New York: Springer-Verlag; 2000. p. 192-205.

Full RJ, Koditschek DE. Templates and anchors: neuromechanical hypotheses of legged locomotion on land. J Exp Biol 1999;202:3325–3332. [PubMed: 10562515]

Full RJ, Kubow T, Schmitt J, Holmes P, Koditschek D. Quantifying dynamic stability and maneuverability in legged locomotion. Integr Comp Biol 2002;42:149–157.

Ghigliazza RM, Altendorfer R, Holmes P, Koditschek D. A simply stabilized running model. SIAM J Appl Dyn Syst 2003;2:187–218.

Gillis GB, Biewener AA. Effects of surface grade on proximal hindlimb muscle strain and activation during rat locomotion. J Appl Physiol 2002;93:1731–1743. [PubMed: 12381761]

Gillis GB, Flynn JP, McGuigan P, Biewener AA. Patterns of strain and activation in the thigh muscles of goats across gaits during level locomotion. J Exp Biol 2005;208:4599–4611. [PubMed: 16326942]

Gorassini MA, Prochazka A, Hiebert GW, Gauthier MJA. Corrective responses to loss of ground support during walking. 1 Intact cats. J Neurophysiol 1994;71:603–610. [PubMed: 8176429]

Grillner S. Locomotion in vertebrates: central mechanisms and reflex interaction. Physiol Rev 1975;55:247–302. [PubMed: 1144530]

Hiebert GW, Gorassini MA, Jiang W, Prochazka A, Pearson KG. Corrective responses to loss of ground support during walking. 2 Comparison of intact and chronic spinal cats. J Neurophysiol 1994;71:611–622. [PubMed: 8176430]

Josephson RK. Dissecting muscle power output. J Exp Biol 1999;202:3369–3375. [PubMed: 10562519]

Kerdok AE, Biewener AA, McMahon TA, Weyand PG, Herr HM. Energetics and mechanics of human running on surfaces of different stiffnesses. J Appl Physiol 2002;92:469–478. [PubMed: 11796653]

Koditschek DE, Full RJ, Buehler M. Mechanical aspects of legged locomotion control. Arthropod Struct Dev 2004;33:251–272. [PubMed: 18089038]

Marsh RL. How muscles deal with real-world loads: the influence of length trajectory on muscle performance. J Exp Biol 1999;202:3377–3385. [PubMed: 10562520]

McMahon TA. The role of compliance in mammalian running gaits. J Exp Biol 1985;115:263–282. [PubMed: 4031769]

McMahon TA, Cheng GC. The mechanics of running: how does stiffness couple with speed? J Biomech 1990;23:65–78. [PubMed: 2081746]

McMahon TA, Valiant G, Frederick EC. Groucho running. J Appl Physiol 1987;62:2326–2337. [PubMed: 3610929]

Moritz CT, Farley CT. Passive dynamics change leg mechanics for an unexpected surface during human hopping. J Appl Physiol 2004;97:1313–1322. [PubMed: 15169748]

Nichols TR, Houk JC. Improvement in linearity and regulation of stiffness that results from actions of stretch reflex. J Neurophysiol 1976;39:119–142. [PubMed: 1249597]

Pandy MG, Kumar V, Berme N, Waldron KJ. The dynamics of quadrupedal locomotion. J Biomech Eng 1988;110:230–237. [PubMed: 3172744]

Pearson K. Motor systems. Curr Opin Neurobiol 2000;10:649–654. [PubMed: 11084328]

Pearson KG, Misiaszek JE, Fouad K. Enhancement and resetting of locomotor activity by muscle afferents. Ann N Y Acad Sci 1998;860:203–215. [PubMed: 9928313]

Roberts TJ. The integrated function of muscles and tendons during locomotion. Comp Biochem Physiol 2002;133A:1087–1099.

Roberts TJ, Scales JA. Adjusting muscle function to demand: joint work during acceleration in wild turkeys. J Exp Biol 2004;207:4165–4174. [PubMed: 15498962]

Roberts TJ, Marsh RL, Weyand PG, Taylor CR. Muscular force in running turkeys: the economy of minimizing work. Science 1997;275:1113–1115. [PubMed: 9027309]

Schmitt J, Holmes P. Mechanical models for insect locomotion: dynamics and stability in the horizontal plane. I Theory. Biol Cybern 2000a;83:501–515. [PubMed: 11130583]

Schmitt J, Holmes P. Mechanical models for insect locomotion: dynamics and stability in the horizontal plane. II Application. Biol Cybern 2000b;83:517–527. [PubMed: 11130584]

Seyfarth A, Geyer H, Gunther M, Blickhan R. A movement criterion for running. J Biomech 2002;35:649–655. [PubMed: 11955504]

Seyfarth A, Geyer H, Herr H. Swing-leg retraction: a simple control model for stable running. J Exp Biol 2003;206:2547–2555. [PubMed: 12819262]

Taga G, Yamaguchi Y, Shimizu H. Self-organized control of bipedal locomotion by neural oscillators in unpredictable environment. Biol Cybern 1991;65:147–159. [PubMed: 1912008]

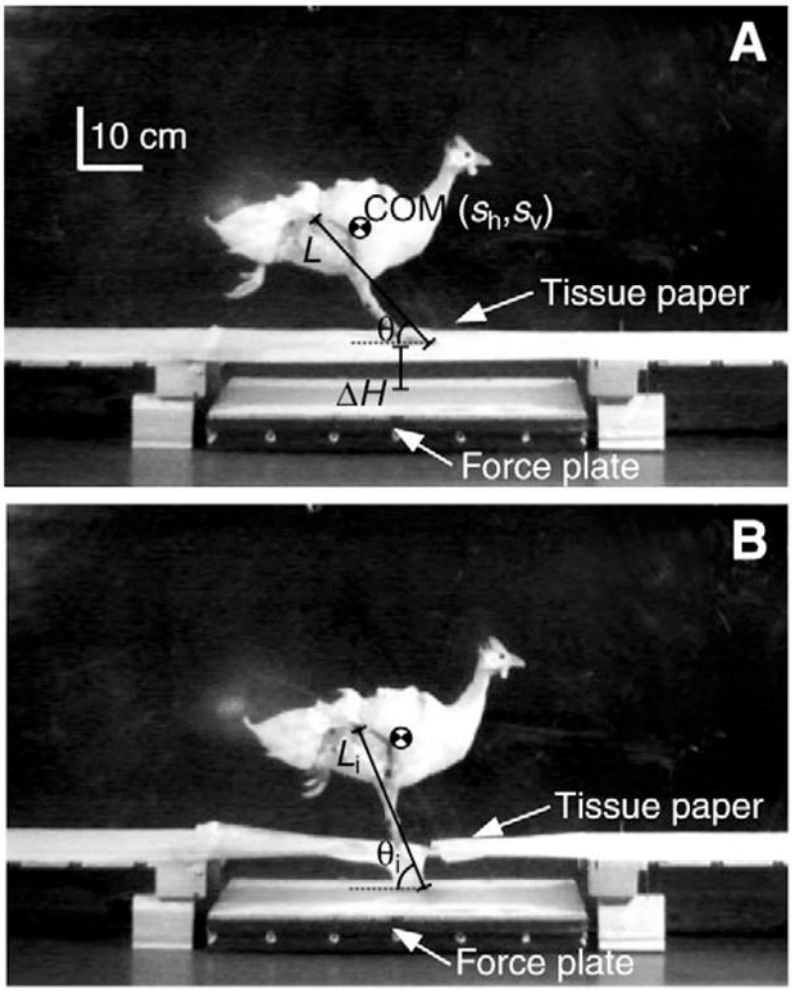

Fig. 1.

Still frames of a guinea fowl during an unexpected perturbation to illustrate experimental set-up. The ground force data reported in this paper were reported previously (Daley et al., 2006), where they were used to calculate changes in mechanical energy of the body center of mass (COM). Here, the experimental data were analyzed further by adding limb kinematics and inverse dynamics to investigate joint mechanics during the perturbation. A 0.6 m long force plate was placed at the midpoint of an 8 m long runway and rested 8.5 cm below the runway surface. White tissue paper pulled tightly across the gap created the appearance of a uniform substrate. Kinematics and ground reaction forces were measured through time (moving from frame A to frame B) for the perturbed step. These data were used to (1) evaluate whole limb mechanics and (2) calculate joint moments and work using inverse dynamics, as described in Materials and methods.

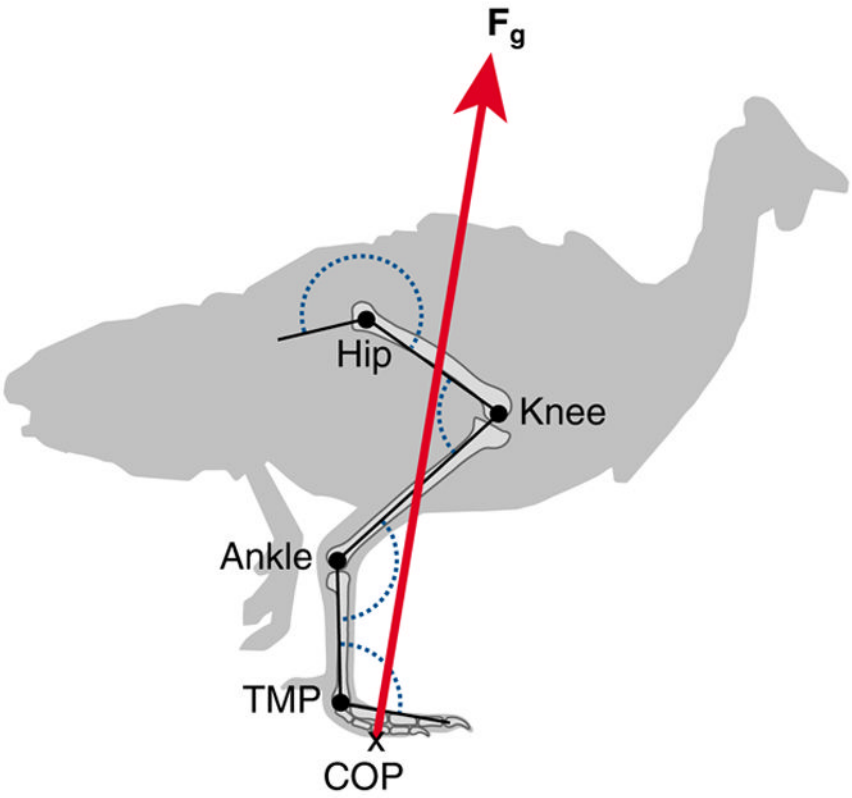

Fig. 2.
Schematic illustration of variables used for calculation of external joint moments and work using inverse dynamics. Joint angles for the hip, knee, ankle and tarsometatarso-phalangeal (TMP) joints are shown in dotted blue. X marks the force-plate center of pressure (COP); red arrow, the ground reaction force vector ($\mathbf{F_g}$). See Materials and methods for further details.

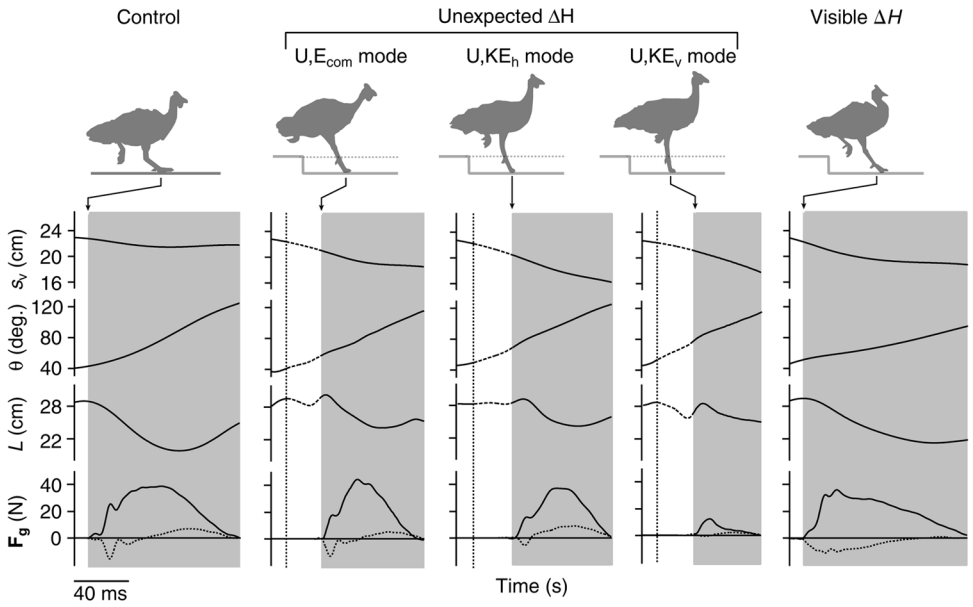

Fig. 3.

COM height (s_v), limb angle relative to horizontal (θ), limb length as the distance between hip and toe (L) and vertical (f_v, solid line) and horizontal (f_h, dotted line) components of ground reaction forces during the C, U and V treatments. The three U trials show typical examples corresponding to the three distinct COM energy response patterns (Daley et al., 2006). Silhouettes illustrate limb posture at the point of ground contact. Dotted line indicates the time of tissue paper contact, and the grey bars indicate duration of ground contact (t_c). Ground reaction forces and COM position data were reported previously (Daley et al., 2006) and are shown here for reference. In the present paper we relate the limb loading and energy patterns to joint mechanics during the step following the perturbation.

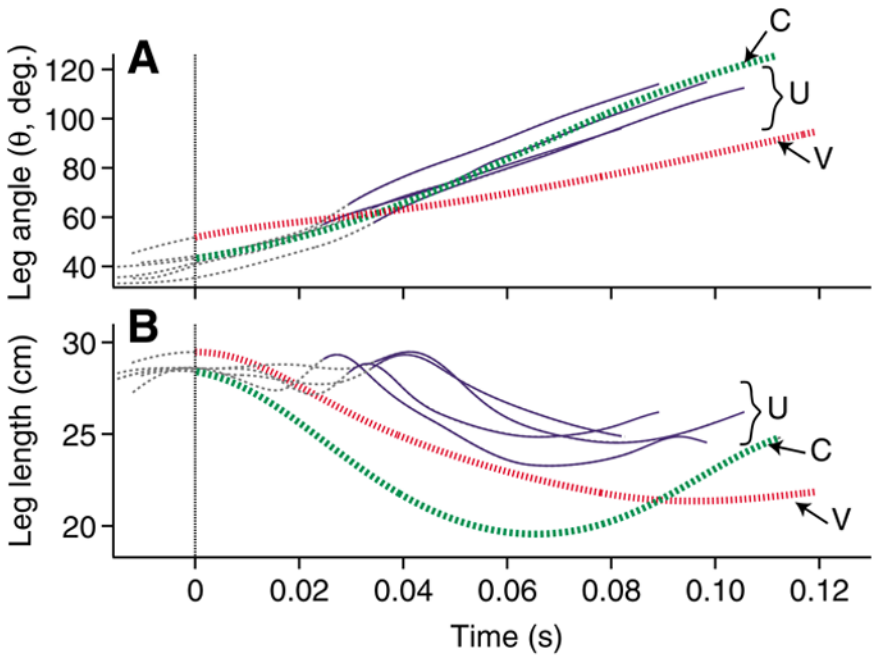

Fig. 4.

(A) Limb angle relative to horizontal (θ) and (B) limb length as the distance between hip and toe (*L*) over the course of the perturbed step for all U trials from one individual (solid blue), with a typical C (broken green) and V (dotted red) trial from the same individual. Thin broken grey lines indicate the aerial phase. Thicker lines indicate the period of ground contact. The dotted vertical line indicates the time of tissue paper contact for U trials, and the time of ground contact for the C and V trials. Data are shown for the period from aerial phase peak in COM height to the end of the stance phase following the perturbation.

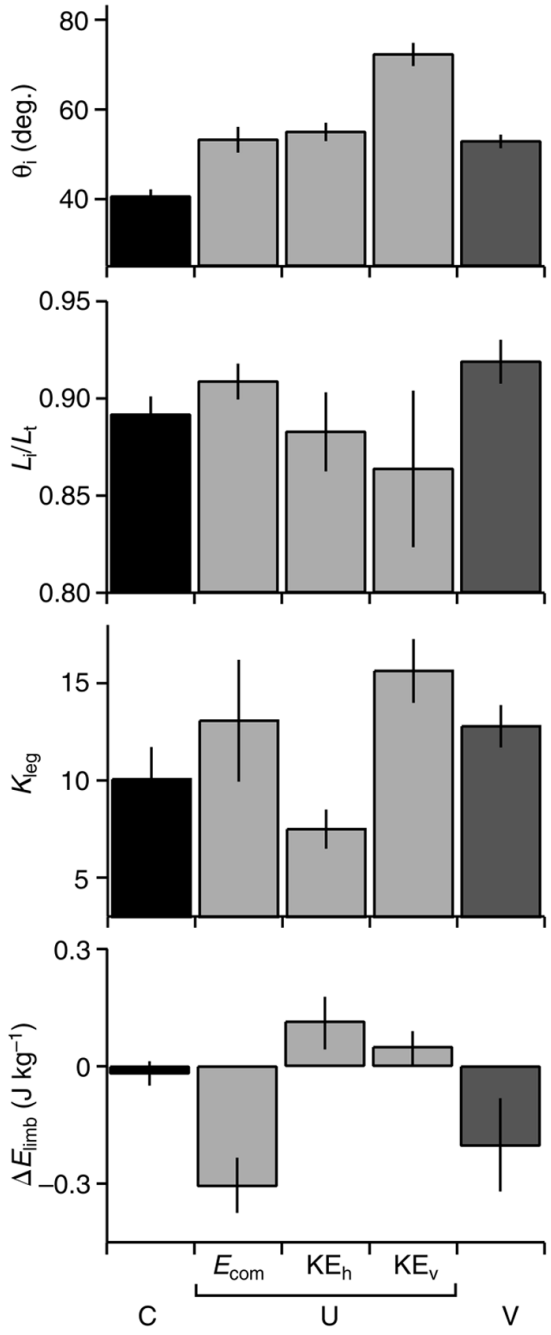

Fig. 5.

Initial limb contact angle (θ_i), initial relative limb length (L_i/L_t), dimensionless limb stiffness (K_{leg}), and net work of the limb during stance (ΔE_{limb}; calculated from inverse dynamics) during C (black), U (light grey) and V (dark grey) treatments with U trials subdivided by response mode. Values are mean ± s.e.m. (N=10, 7, 9, 3, 10 for the respective categories).

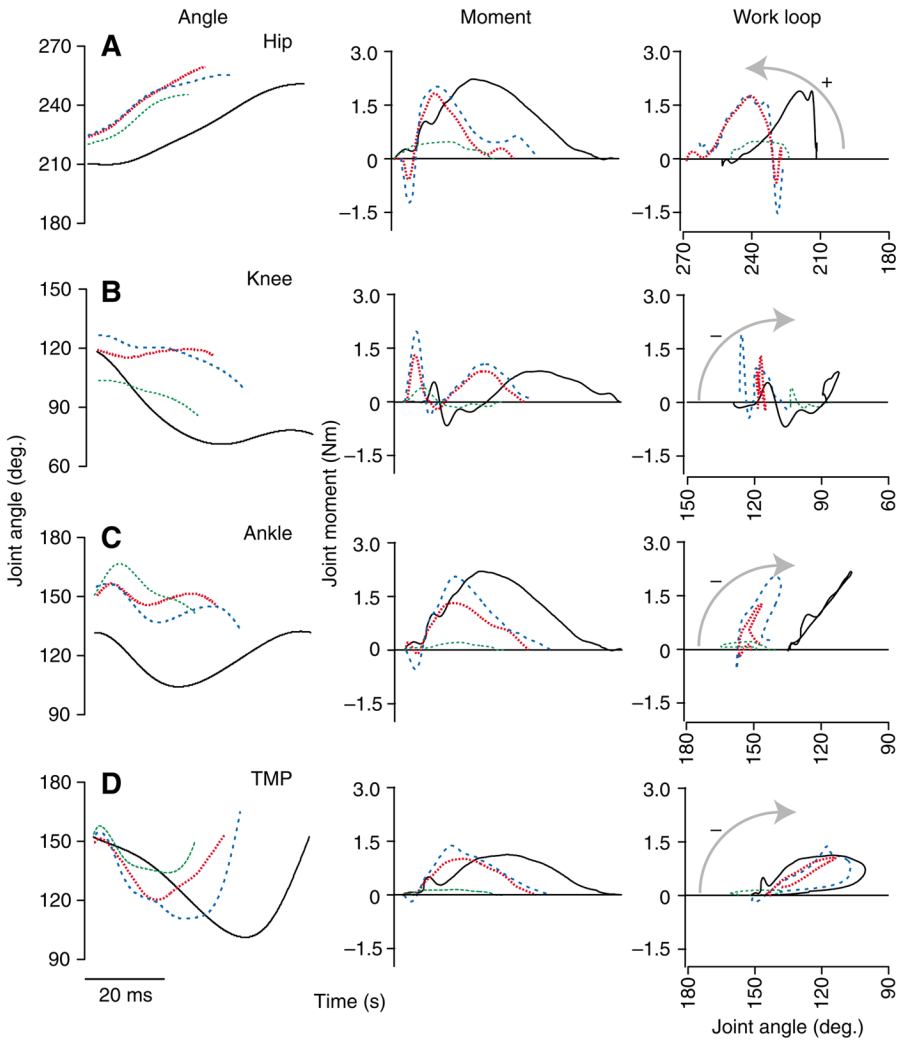

Fig. 6.

Joint mechanics during stance. Joint angles (left), external moments (middle) and joint work loops (moment–angle plots, right) over the course of stance for the hip (A), knee (B), ankle (C) and TMP (D). A representative U trial for each of the 3 response modes is shown (broken colored lines) with a level running trial for comparison (C, solid black line). Increasing joint angles indicate extension, and positive moments indicate extensor moments. Arrows indicate the direction of work loops. Counter-clockwise indicates energy production by the joint, clockwise indicates energy absorption.

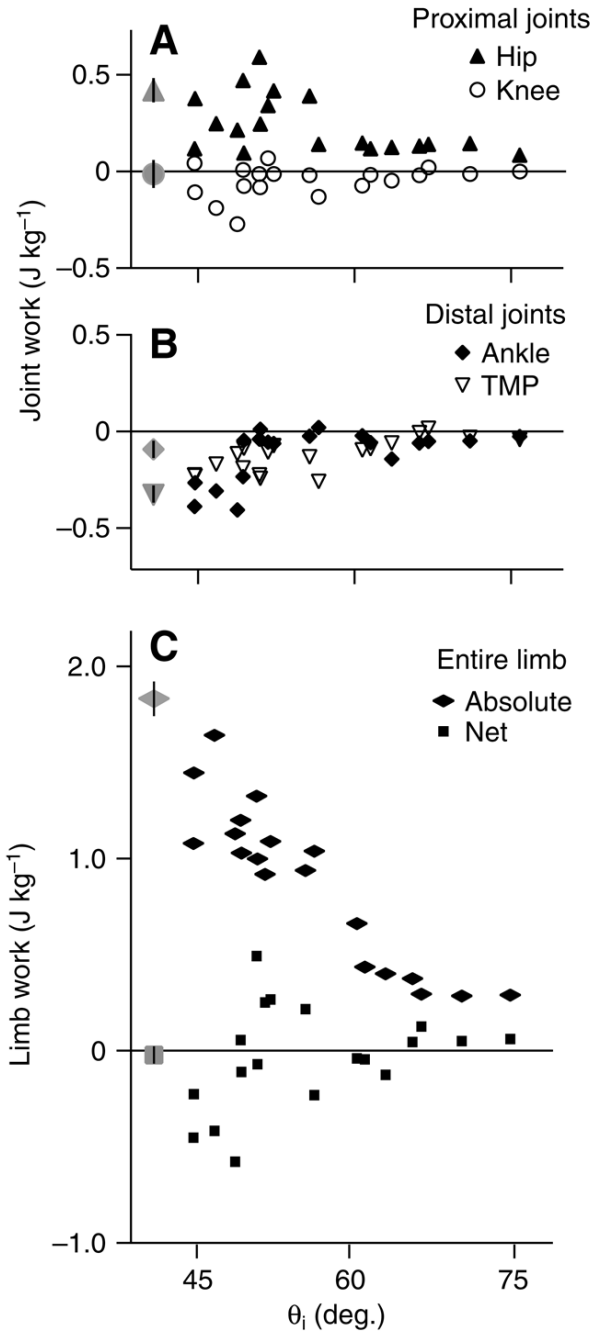

Fig. 7.

Net external mechanical work in relation to limb contact angle (θ_i) for (A) the hip and knee, (B) the ankle and TMP and (C) the entire limb. Black symbols are individual U trials, grey symbols show the mean ± s.e.m. for C trials (*N*=10).

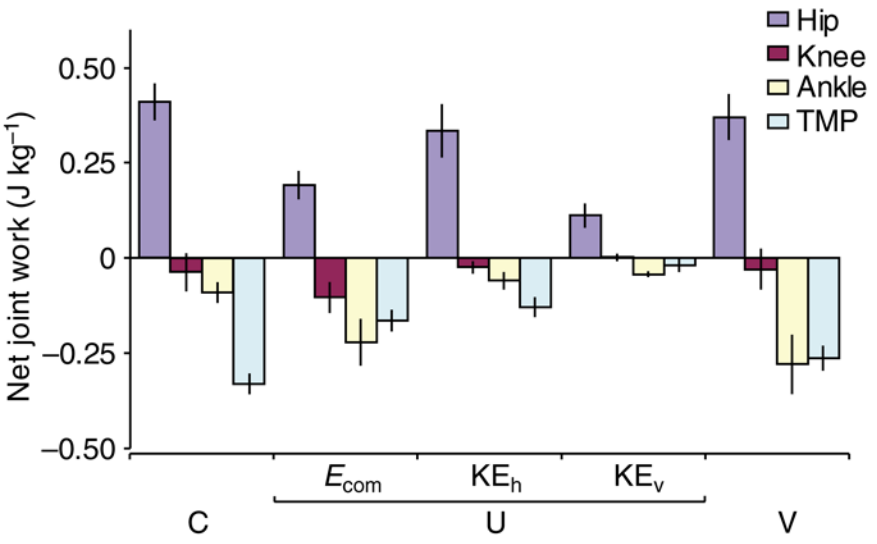

Fig. 8.

Net work at each joint during C (level running), U (unexpected drop) and V (visible drop) trials with U trials subdivided by response mode. Values are mean ± s.e.m. (*N*=10, 7, 9, 3, 10, for the respective categories).

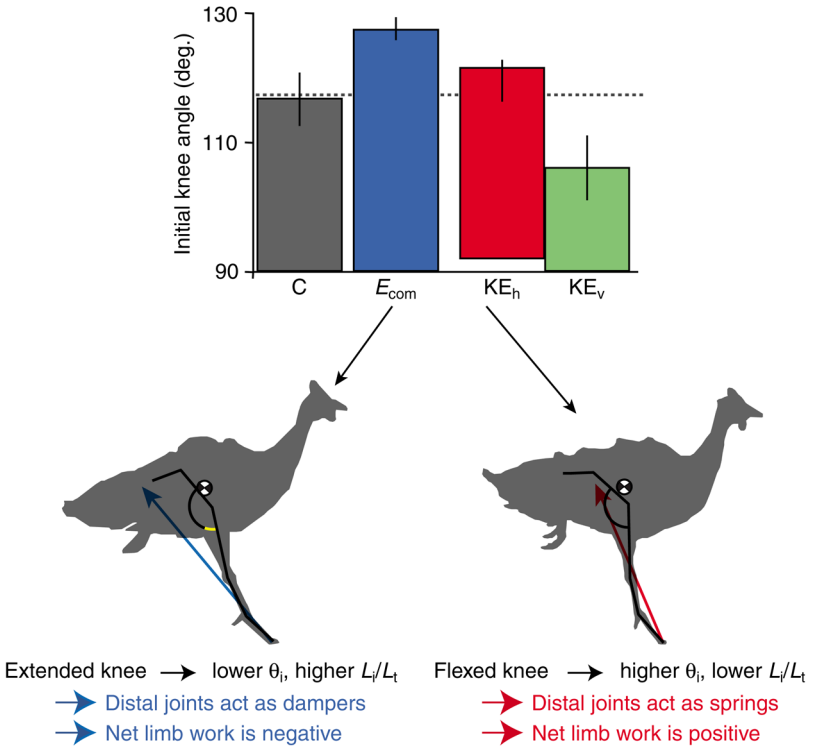

Fig. 9.

Initial stance phase knee angle determines limb posture and the work balance among the joints. The knee angle is the only joint angle that differs significantly at the onset of ground contact among the U response modes. If the knee is extended at contact (left silhouette) the limb has a lower initial angle and longer initial length. This extended posture is associated with larger decelerating forces, greater energy absorption by the ankle and TMP, and net energy absorption by the limb. If the knee is flexed at contact (right silhouette), the limb has a higher initial angle and shorter initial length. This flexed posture is associated with lower decelerating forces, spring-like function of the ankle and TMP, and net energy production by the limb. In cases with an extremely flexed knee, the distal limb simply collapses without supporting substantial weight (KE_v mode, silhouette not shown). Values are mean ± s.e.m. (N=10, 7, 9, 3, for the respective categories).

Table 1

Subject data: mass, sum of limb segment lengths, standing hip height and number of trials

Individual	Mass (kg)	L_t (m)	*HH* (m)	Trials		
				C	U	V
1	1.10	0.31	0.19	2	5	2
2	1.52	0.32	0.20	2	4	2
3	2.06	0.33	0.20	2	2	3
4	2.41	0.37	0.22	2	3	2
5	2.64	0.37	0.22	2	5	1

For abbreviations, see List of symbols and abbreviations.

Table 2

Mixed model ANOVA for effect of individual and‘ behavior category’ on limb parameters

	Individual			‘Behavior category’		
Variable	**d.f.**	***F***	***P***	**d.f.**	***F***	***P***
L_i/L_t	4,18	3.479	0.028	3,12	4.74	**0.021**
K_{leg}	4,18	9.57	**<0.001**	3,12	2.352	0.11
θ_i	4,18	1.786	0.176	3,12	11.06	**0.001**
$\Delta\theta/\Delta T_c$	4,18	2.327	0.096	3,12	11.743	**0.001**

‘Behavior category’: C, U_{Ecom}, U_{KEh}, U_{KEv}, V; see List of symbols and abbreviations.

Bold type indicates statistical significance at the α=0.05 level after sequential Bonferroni correction.